Molecular Plant
Research Article

CellPress
PARTNER JOURNAL

Antagonism of Transcription Factor MYC2 by EDS1/PAD4 Complexes Bolsters Salicylic Acid Defense in Arabidopsis Effector-Triggered Immunity

Haitao Cui[1,3,4], Jingde Qiu[1,4], Yue Zhou[2], Deepak D. Bhandari[1], Chunhui Zhao[3], Jaqueline Bautor[1] and Jane E. Parker[1,*]

[1]Department of Plant-Microbe Interactions, Max-Planck Institute for Plant Breeding Research, Carl-von-Linné Weg 10, 50829 Cologne, Germany

[2]Department of Plant Developmental Biology, Max-Planck Institute for Plant Breeding Research, 50829 Cologne, Germany

[3]Key Laboratory of Ministry of Education for Genetics, Breeding and Multiple Utilization of Crops, Plant Immunity Center, Fujian Agriculture University, Fuzhou 350002, China

[4]These authors contributed equally to this article.

***Correspondence: Jane E. Parker (parker@mpipz.mpg.de)**

https://doi.org/10.1016/j.molp.2018.05.007

ABSTRACT

In plant immunity, pathogen-activated intracellular nucleotide binding/leucine rich repeat (NLR) receptors mobilize disease resistance pathways, but the downstream signaling mechanisms remain obscure. Enhanced disease susceptibility 1 (EDS1) controls transcriptional reprogramming in resistance triggered by Toll-Interleukin1-Receptor domain (TIR)-family NLRs (TNLs). Transcriptional induction of the salicylic acid (SA) hormone defense sector provides one crucial barrier against biotrophic pathogens. Here, we present genetic and molecular evidence that in Arabidopsis an EDS1 complex with its partner PAD4 inhibits MYC2, a master regulator of SA-antagonizing jasmonic acid (JA) hormone pathways. In the TNL immune response, EDS1/PAD4 interference with MYC2 boosts the SA defense sector independently of EDS1-induced SA synthesis, thereby effectively blocking actions of a potent bacterial JA mimic, coronatine (COR). We show that antagonism of MYC2 occurs after COR has been sensed inside the nucleús but before or coincident with MYC2 binding to a target promoter, *pANAC019*. The stable interaction of PAD4 with MYC2 *in planta* is competed by EDS1-PAD4 complexes. However, suppression of MYC2-promoted genes requires EDS1 together with PAD4, pointing to an essential EDS1-PAD4 heterodimer activity in MYC2 inhibition. Taken together, these results uncover an immune receptor signaling circuit that intersects with hormone pathway crosstalk to reduce bacterial pathogen growth.

Key words: NLR receptor, stress hormone network, *Pseudomonas syringae*, AvrRps4, RRS1/RPS4, *coi1*

Cui H., Qiu J., Zhou Y., Bhandari D.D., Zhao C., Bautor J., and Parker J.E. (2018). Antagonism of Transcription Factor MYC2 by EDS1/PAD4 Complexes Bolsters Salicylic Acid Defense in Arabidopsis Effector-Triggered Immunity. Mol. Plant. **11**, 1053–1066.

INTRODUCTION

Intracellular recognition of pathogen molecules by plant and animal nucleotide binding domain-leucine rich repeat (NLR) receptors is a crucial innate immunity mechanism for inducing local and systemic anti-microbial pathways (Jones et al., 2016). In plants, NLRs recognize actions of specific pathogen virulence factors (known as effectors) delivered to host cells to manipulate cellular processes and promote disease. Like their mammalian counterparts, plant NLR proteins evolved as ATP-driven molecular switches and, in both systems, building NLR homo- or hetero-complexes is necessary for receptor function (Jones et al., 2016).

Two major plant NLR classes differ principally in their N-terminal domains: CC-NLRs (CNLs) have a coiled-coil domain and TIR-NLRs (TNLs) have a Toll-Interleukin1-Receptor signaling (TIR) domain. These N-termini not only participate in maintaining

Published by the Molecular Plant Shanghai Editorial Office in association with Cell Press, an imprint of Elsevier Inc., on behalf of CSPB and IPPE, SIBS, CAS.

closed, pre-activated NLR complexes but also in downstream signaling (Maekawa et al., 2011; Cui et al., 2015; Zhang et al., 2017). TNL or CNL recognition of pathogen effectors leads to rapid transcriptional reprogramming of anti-microbial and stress hormone pathways, often accompanied by host cell death, in a process called effector-triggered immunity (ETI) (Cui et al., 2015; Tsuda and Somssich, 2015). ETI also involves a reorganization of nuclear-cytoplasmic trafficking (Cheng et al., 2009; Gu et al., 2016). Some NLRs function in nuclei and interact with transcription factors (TFs) (Cui et al., 2015). How NLRs signal in ETI to stop pathogen growth is not resolved.

EDS1 is an essential transducer of TNL signals in resistance to biotrophic and hemi-biotrophic pathogens (Wiermer et al., 2005), and encodes a lipase-like nucleocytoplasmic protein whose nuclear accumulation is necessary for transcriptional defense reprogramming in Arabidopsis TNL ETI and autoimmunity (Wirthmueller et al., 2007; Cheng et al., 2009; Garcia et al., 2010; Stuttmann et al., 2016). Evidence of EDS1 association with several nuclear TNLs (Bhattacharjee et al., 2011; Heidrich et al., 2011; Kim et al., 2012; Huh et al., 2017), suggests that it serves as a bridge between TNLs and the transcriptional machinery. Arabidopsis EDS1 and its sequence-related direct partners PAD4 and SAG101 (senescence associated gene 101) possess a unique fusion between an N-terminal α/β hydrolase (lipase-like) domain and a C-terminal α-helical bundle (referred to as 'EP') domain (Feys et al., 2005; Wagner et al., 2013). EDS1/PAD4 or EDS1/SAG101 heterodimers, formed via interfaces in the partner N-terminal domains, signal in TNL ETI (Wagner et al., 2013). Few other plant ETI early signaling components have been isolated from forward genetic screens. This is likely due to functional redundancy, as shown for several transcription factor families (Zhu et al., 2010; Padmanabhan et al., 2013; Kim et al., 2014; Jacob et al., 2018). Also, it is increasingly clear that compensatory mechanisms buffer certain defense sectors against pathogen or genetic interference (Cui et al., 2017; Hillmer et al., 2017). This increases stress network resilience but can obscure individual pathway contributions.

The biotic stress hormone salicylic acid (SA) is important for immunity against biotrophic pathogens. Transcriptional induction of the major SA biosynthesis gene *isochorismate synthase 1* (*ICS1*) increases SA accumulation (Wildermuth et al., 2001), and SA signaling via the transcriptional co-activator NPR1 (nonexpresser of PR genes 1) promotes local and systemic resistance (Fu and Dong, 2013). Antagonism between SA and jasmonic acid (JA)-induced pathways involved in resistance against necrotrophic pathogens, enables exquisite tuning of host responses (Pieterse et al., 2009; Zheng et al., 2012; Van der Does et al., 2013). Disabling of SA signaling by pathogen virulent factors such as the bacterial JA mimic coronatine (COR) and effectors, often through manipulation of JA-stimulated pathways (Brooks et al., 2005; Kazan and Lyons, 2014; Yang et al., 2017), underscores the importance of SA in plant immunity.

In TNL ETI, *ICS1* expression and SA accumulation are boosted by *EDS1*/*PAD4* in a positive feedback loop (Jirage et al., 1999; Wiermer et al., 2005). Strikingly, *EDS1*/*PAD4* are able to induce SA-responsive gene expression and pathogen resistance independently of *ICS1*-generated SA, indicating a compensatory mechanism in ETI (Cui et al., 2017). Here, we describe an *ICS1*-independent, nuclear EDS1/PAD4 function in TNL ETI that antagonizes MYC2, a transcriptional master regulator of JA signaling (Kazan and Manners, 2013). EDS1/PAD4 inhibition of MYC2 interrupts SA pathway interference by COR. Our data reveal a new signaling intersection between ETI and the plant host stress hormone network, which leads to bacterial resistance.

RESULTS

Mutations in *COI1* Partially Restore Bacterial Resistance in *eds1-2*

We performed a genetic screen for restored TNL resistance in ethane methyl sulfonate (EMS)-mutagenized Arabidopsis *eds1-2* plants (accession Columbia-0, Col), anticipating that this might uncover new factors that are repressed in TNL immunity. In Col, COR-producing *P. syringae* pv *tomato* strain DC3000 expressing the Type-III secreted effector *AvrRps4* (*Pst AvrRps4*) is recognized by a nuclear TNL receptor pair RRS1-S (resistant to *Ralstonia solanacearum* 1)/RPS4 (resistant to *P. syringae* 4) (Heidrich et al., 2011; Saucet et al., 2015). RRS1-S/RPS4 confer bacterial resistance and gene expression changes accompanied by a weak host cell death response (Heidrich et al., 2011, 2013; Narusaka et al., 2016). *Pst AvrRps4* was spray-inoculated onto 2-week-old M2-generation *eds1-2* seedlings in soil. At 5–6 d after inoculation, *eds1-2* plants were chlorotic or dead while Col wild-type plants remained green (Figure 1A). In a screen of ~650,000 M2 plants representing ~20,000 M1 individuals, we identified 12 independent mutations in *coronatine insensitive 1* (*COI1*) (Supplemental Table 1). *COI1* encodes an F-box protein co-receptor with JAZ (jasmonate-zim-domain) repressors that binds bioactive JA-isoleucine (JA-Ile) or COR to initiate plant JA responses (Sheard et al., 2010). Two new recessively inherited amino acid exchange mutations in the COI1 LRR domain (Supplemental Figure 1A), denoted here as *coi1-41* and *coi1-42*, were partially fertile (Supplemental Table 1) and therefore used in further genetic analysis. *Coi1-41* and *coi1-42* are G/A transitions resulting in E361K and A384T exchanges, respectively. Based on the Arabidopsis COI1 crystal structure (Sheard et al., 2010), *coi1-41* is located outside the ASK1 (arabidopsis skp1 homologue 1)-binding region and the JA-Ile/COR-binding pocket. By contrast, *coi1-42* is located in the JA-Ile/COR-binding pocket at the same site as an A384V exchange reducing COI1 sensitivity to COR but not JA-Ile (Zhang et al., 2015).

After backcrossing *coi1-41* and *coi1-42* with *eds1-2*, the effect of the *coi1-41* and *coi1-42* mutations on COR application (0.2 μM) was measured in seedling root growth inhibition assays. *Eds1-2 coi1-42* was as insensitive as the Col *coi1-1* null mutant, whereas *eds1-2 coi1-41* exhibited slight sensitivity to COR (Supplemental Figure 1B). Therefore, plants harboring the *coi1-41* or *coi1-42* mutations in an *eds1-2* background have strongly reduced COR responsiveness.

Isolation of multiple *coi1* alleles in the *eds1-2* screen (Supplemental Table 1) suggested that TNL/EDS1 pathway activation dampens *Pst AvrRps4* COR-induced disease susceptibility. Because *COI1*

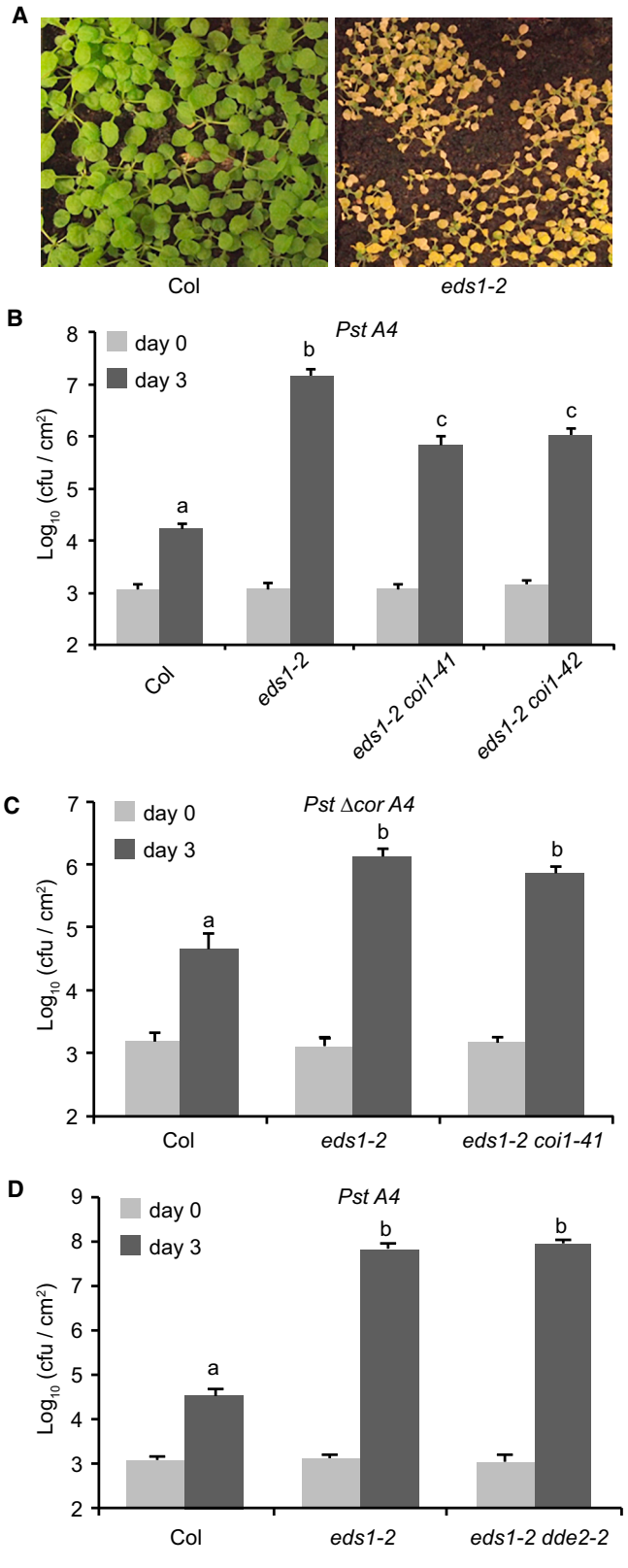

Figure 1. Mutation in *COI1* Reduces *eds1-2* Susceptibility to *Pst AvrRps4*.

(A) Arabidopsis Col and *eds1-2* disease symptoms after *Pst AvrRps4* (*Pst A4*) infection. Two-week-old seedlings grown in soil were spray inoculated with *Pst A4* (OD_{600} = 0.2). Picture taken at 6 dpi.

(B–D) Growth of *Pst A4* **(B and D)** or COR deficient strain *Pst Δcor A4* **(C)** in leaves of the indicated genotypes. Four-week-old plants were infiltrated with bacterial suspensions (OD_{600} = 0.0002) and bacterial titers were determined at 0 and 3 dpi. Error bars indicate means + SDs (the number of biological replicates in one experiment was n = 4 for day 0 and n = 6 for day 3). Different letters indicate statistical significance ($p < 0.01$) determined by one-way ANOVA with multiple comparison correction using Tukey's HSD. Experiments were repeated at least twice with similar results.

is required for COR stimulated re-opening of stomata, which increases bacterial leaf entry (Melotto et al., 2006), we infiltrated *Pst AvrRps4* directly into leaves of *eds1-2 coi1-41* and *eds1-2 coi1-42* to bypass stomatal effects and measured bacterial titers at 3 d post infiltration (dpi). *Pst AvrRps4* growth in *eds1-2 coi1-41* and *eds1-2 coi1-42* leaves was intermediate between that of resistant Col and susceptible *eds1-2* plants (Figure 1B). Therefore, *coi1* mutations in *eds1-2* increase post-stomatal immunity to *Pst AvrRps4*. Testing growth of a COR-deficient strain *Pst Δcor AvrRps4* (Cui et al., 2017) infiltrated into *eds1-2 coi1-41* showed that bacterial COR accounts for the difference in *Pst AvrRps4* growth between *eds1-2* and *eds1-2 coi1-41* (Figure 1C). There was no difference in *Pst AvrRps4* growth in Col and a double mutant line generated between *eds1-2* and the endogenous JA biosynthetic mutant, *dde2-2* (*delayed-dehiscence2-2*) (Figure 1D). We concluded that increased bacterial growth in *eds1-2* is largely due to *Pst AvrRps4* COR signaling via the JA receptor COI1.

TNL/EDS1 Immunity Dampens COR Stimulated JA Pathway Gene Expression

We examined whether *EDS1* negatively regulates JA/COI1-controlled gene expression in TNL (*RRS1-S/RPS4*) immunity to *Pst AvrRps4*. JA responses separate into two major pathways downstream of COI1. The bHLH TF MYC2 and its two homologs MYC3 and MYC4 induce MYC2-branch genes, including *VSP1* (*vegetative storage protein 1*) and *JAZ10* (*jasmonate zim-domain protein 10*) (Pieterse et al., 2009; Fernandez-Calvo et al., 2011). The bZIP TFs ERF1 (ethylene response factor 1) and ORA59 (octadecanoid-responsive ap2/erf 59) induce ERF-branch genes, for example *PDF1.2* (*plant defensin 1.2*). ORA59 and ERF1 are directly repressed by MYC2 (Zhai et al., 2013). We quantified *VSP1*, *JAZ10* and *PDF1.2* transcripts by qRT-PCR in Col and *eds1-2* leaves at 0, 8 and 24 h after *Pst* AvrRps4 infiltration and detected higher expression of these genes in *eds1-2* compared with Col at 8 hpi and, more obviously, at 24 hpi (Figure 2A). Differences in *VSP1* and *JAZ10* expression between *eds1-2* and Col were not observed at 24 hpi with *Pst Δcor AvrRps4* (Figure 2B). In a published microarray data set generated from *Pst AvrRps4*-infiltrated leaves (OD_{600} = 0.01) at 6 hpi (Bartsch et al., 2006) expression of ~30 JA-responsive genes, including markers of JA-signaling (*PDF1.2*, *VSP1, THI2.1*) and several *JAZs* (*JAZ2, JAZ3, JAZ6, JAZ7, JAZ9* and *JAZ10*), was higher in *eds1-2* than Col (Figure 2C and Supplemental Table 2). Together, these data suggest that EDS1 antagonizes bacterial COR-promoted JA pathway gene expression in TNL immunity.

VSP1, *JAZ10*, and *PDF1.2* expression at 24 hpi with *Pst AvrRps4* (Figure 2D) was similar between *eds1-2* and a Col *rrs1s/rrs1b* mutant that fails to recognize *AvrRps4* (Saucet et al., 2015),

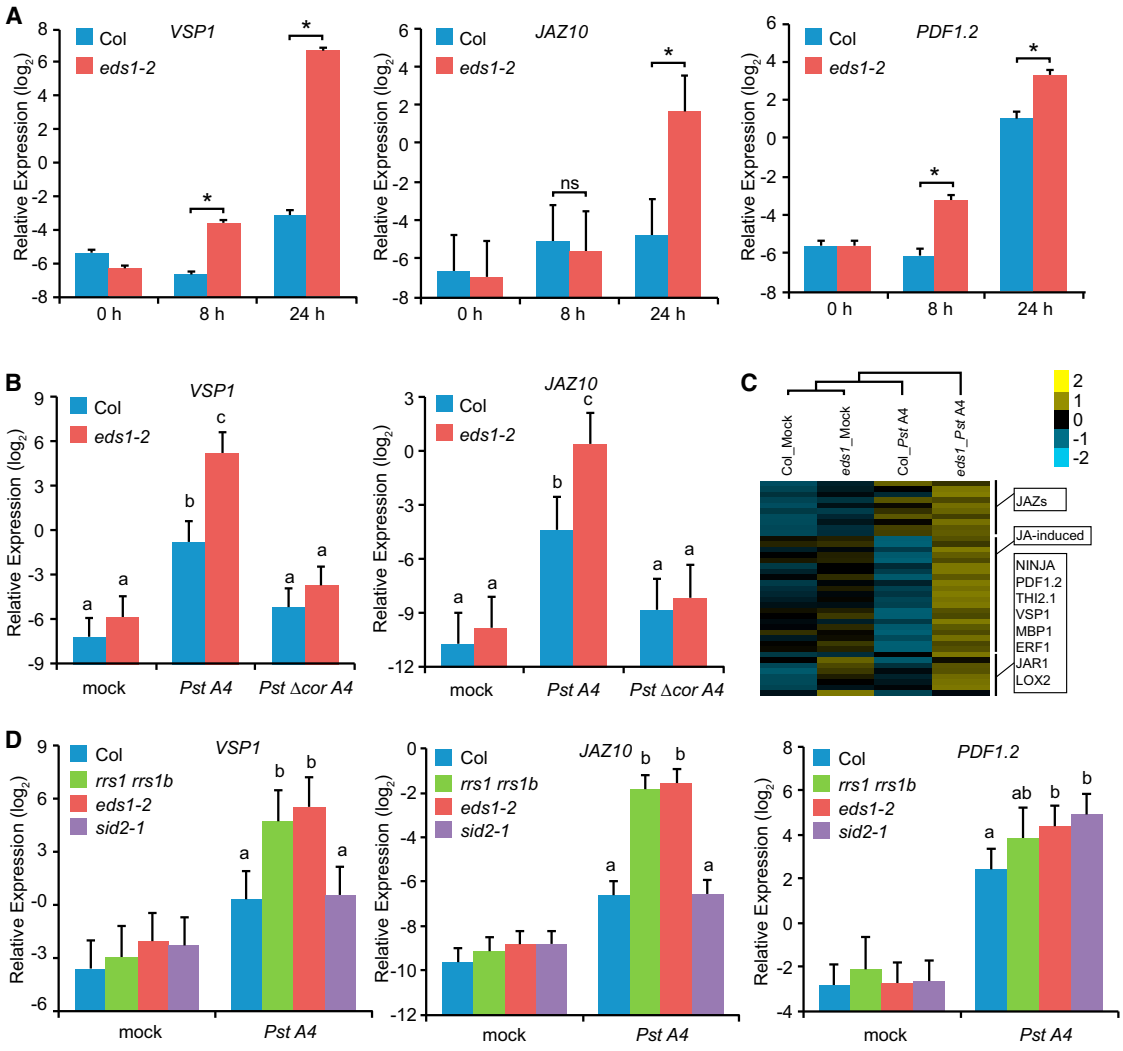

Figure 2. TNL/EDS1 Signaling Suppresses the Expression of COR-Induced JA Pathway Genes.

(A) *VSP1*, *JAZ10* and *PDF1.2* expression in Col and *eds1-2* plants at 0, 8, and 24 h post infiltration (hpi) with *Pst AvrRps4*, measured by qRT-PCR. Four-week-old plants were infiltrated with a bacterial suspension (OD_{600} = 0.002).

(B) *VSP1* and *JAZ10* expression in Col and *eds1-2* plants at 24 h hpi with the mock control (H_2O), *Pst AvrRps4* (*Pst A4*) or *Pst Δcor A4*, measured by qRT-PCR.

(C) Heatmap representing the expression patterns of 39 JA-induced genes in Col or *eds1-2* at 6 h after infiltration with *Pst AvrRps4* (*Pst A4*) or H_2O (mock) in a microarray data set (E-MEXP-546, http://www.ebi.ac.uk/arrayexpress/) (Bartsch et al., 2006). Gene expression values were log_2 transformed and normalized using Gene Cluster software, and visualized using Freeview software (Eisen et al., 1998). JA-induced genes were selected using the Genevestigator tool (see Methods).

(D) *VSP1*, *JAZ10* and *PDF1.2* expression in Col, *rrs1a/b, eds1-2* or *sid2-1* plants at 24 hpi with mock (H_2O) or *Pst A4* treatment, measured by qRT-PCR.

(B and D) Leaves of 4-week-old plants were infiltrated with *Pst A4* (OD_{600} = 0.002).

For qRT-PCR analyses in **A**, **B**, and **D**, gene expression was normalized to *AT4G26410* and is shown as log_2-transformed data. Bars represent means + SEs calculated from three independent experiments (three biological replicates) using a mixed linear model (see Methods); * and different letters indicate statistically significant differences with adjusted *p*-value < 0.01 using the Benjamini–Hochberg method for multiple hypothesis testing; ns, not significant.

indicating that TNL (*RRS1-S/RPS4*) activation is necessary for antagonism of JA responses. We then investigated whether SA production is required for *EDS1* inhibition of either or both JA/COI1 signaling branches. Mutation of *ICS1* in the *sid2-1* (*salicylic acid induction deficient 2*) background (Wildermuth et al., 2001) did not affect *EDS1* interference with the expression of COR-stimulated MYC2-branch genes *VSP1* and *JAZ10* in TNL ETI (Figure 2D). By contrast, expression of the ERF-branch marker gene *PDF1.2* was higher in both *eds1-2* and *sid2-1* than in Col (Figure 2D). Therefore, TNL/EDS1 signaling negatively regulates the MYC2-branch independently of *ICS1*, as depicted in Supplemental Figure 2A.

Interference with MYC2-controlled gene expression in TNL/EDS1 immunity might be due to reduced bacterial COR production. Indeed, expression of bacterial COR biosynthesis genes was reduced at 6 h after *Pst AvrRps4* inoculation of Col leaves (Nobori et al., 2018). We therefore tested whether TNL/EDS1

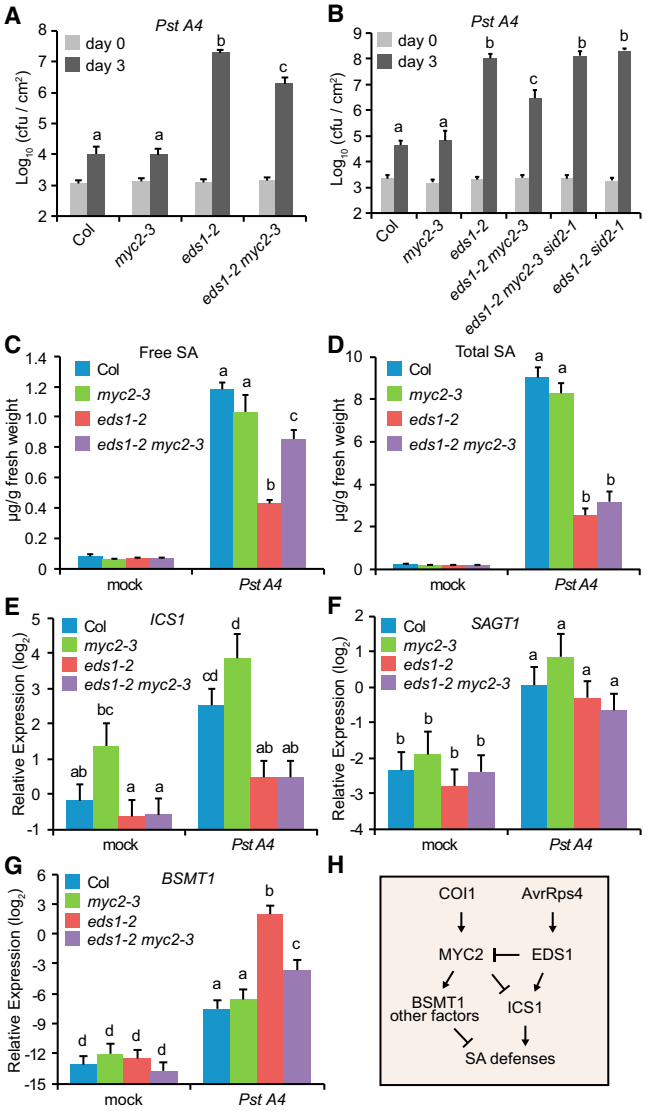

Figure 3. EDS1 Dampens MYC2 Antagonism of SA Resistance in TNL Immunity.

(A and B) *Pst AvrRps4* (*Pst A4*) growth in leaves of the indicated Arabidopsis genotypes at 0 and 3 dpi. Four-week-old plants were infiltrated with bacterial suspensions (OD_{600} = 0.0002) and bacterial titers were determined. Error bars indicate means + SDs (the number of biological replicates in one experiment was n = 4 for day 0 and n = 6 for day 3). Different letters indicate statistical significance (p < 0.01) determined by one-way ANOVA with multiple comparison correction by Tukey HSD. Experiments were repeated twice with similar results.

(C and D) Quantitation of free **(C)** and total **(D)** SA in 4-week-old plants of the indicated Arabidopsis genotypes. Leaf samples were harvested at 24 h after mock (H_2O) or *Pst A4* treatment. Bars represent mean + SDs (n = 3 biological replicates in one experiment). Letters indicate statistical differences (p < 0.05) in one-way ANOVA with multiple comparison correction by Tukey HSD. Three independent experiments gave similar results.

(E–G) Expression of the SA synthesis gene *ICS1* **(E)** and SA metabolic genes *SAGT1* **(F)** and *BSMT1* **(G)** in leaves of the same genotypes as **(C and D)**, measured by qRT-PCR. Gene expression was normalized to *AT4G26410*. Bars represent means + SEs calculated from four **(E and F)** and five **(G)** independent experiments (each containing one biological replicate) using a mixed linear model; different letters indicate statistically significant differences with adjusted p-value < 0.01 using the Benjamini–Hochberg method for multiple hypothesis testing.

(H) Working model for EDS1 antagonism of MYC2 to bolster SA defenses in TNL ETI.

signaling antagonizes exogenous COR-stimulated JA pathways by spraying 0.2 µM COR onto 3-week-old plants of a TNL *RPS4* over-expression (*OE-RPS4*) line, which exhibits *EDS1*-dependent autoimmunity at 22°C (Heidrich et al., 2013). The MYC2 transcriptional response in *OE-RPS4* at 4 h after COR or mock treatments was compared with the response in *OE-RPS4 eds1-2* and *OE-RPS4 sid2-1* lines, as well as in Col, *eds1-2*, and *sid2-1* single mutants by performing qRT-PCR assays. Relative to Col, COR-induced *VSP1* and *JAZ10* gene expression was lower in leaves of *OE-RPS4* and *OE-RPS4 sid2-1* but not *OE-RPS4 eds1-2*, consistent with *EDS1*-driven, *ICS1*-independent antagonism of the MYC2-branch (Supplemental Figure 2B). These data suggest that TNL/EDS1 immunity can interfere with COR-stimulated JA signaling after COR molecules have entered and been sensed by host cells.

COR Stimulates MYC2-Dependent Disease Susceptibility in *eds1-2*

We interrogated TNL/EDS1 antagonism of the MYC2-branch further because it represents a new intersection of ETI with JA response pathways (Supplemental Figure 2A). First, we investigated whether *MYC2* contributes to *Pst AvrRps4* susceptibility in *eds1-2* by crossing *eds1-2* with the null *myc2-3* mutant (Shin et al., 2012). *Pst AvrRps4* growth after leaf infiltration was similar between *eds1-2 myc2-3* and *eds1-2 coi1-41* (Figure 3A), indicating that *MYC2* is a major component of *COI1*-promoted post-stomatal susceptibility in *eds1-2*. An *eds1-2 myc2-3 sid2-1* triple mutant supported similarly high levels of *Pst AvrRps4* growth as *eds1-2* (Figure 3B), indicating that *ICS1*-generated SA accounts for the partially restored resistance in *eds1-2 myc2-3*. The *myc2-3* single mutant plants were fully resistant to *Pst AvrRps4*, consistent with dampening of MYC2 gene regulation in TNL ETI. We concluded that TNL/EDS1 signaling antagonizes the COI1/MYC2 JA branch in ETI, thereby interrupting MYC2 suppression of SA resistance.

COR was reported to lower SA accumulation by repressing *ICS1* and stimulating expression of the SA-converting genes *BSMT1* (*SA methyl transferase 1*) and *SAGT1* (*SA glucosyl transferase gene 1*) through direct MYC2 regulation of the NAC (*Petunia* NAM and Arabidopsis ATAF1, ATAF2, and CUC2) TFs ANAC019, ANAC055 and ANAC072 (Zheng et al., 2012). Increased BSMT1 and SAGT1 enzymatic activities convert pools of active, free SA to the inactive molecules methyl-SA and SA-hexose conjugates, respectively (Zheng et al., 2012). We measured total and free SA levels in Col, *eds1-2, myc2-3* and *eds1-2 myc2-3* plants at 24 hpi with *Pst AvrRps4*. Consistent with the enhanced resistance of *eds1-2 myc2-3* compared with *eds1-2* (Figure 3A), *eds1-2 myc2-3* plants accumulated higher levels of free SA than *eds1-2* (Figure 3C). Total SA levels were similar in the two lines (Figure 3D). *Pst AvrRps4*-induced *ICS1* expression was high in both Col and *myc2-3* but remained low in *eds1-2* and *eds1-2 myc2-3* (Figure 3E). These data suggest that induced *ICS1* expression

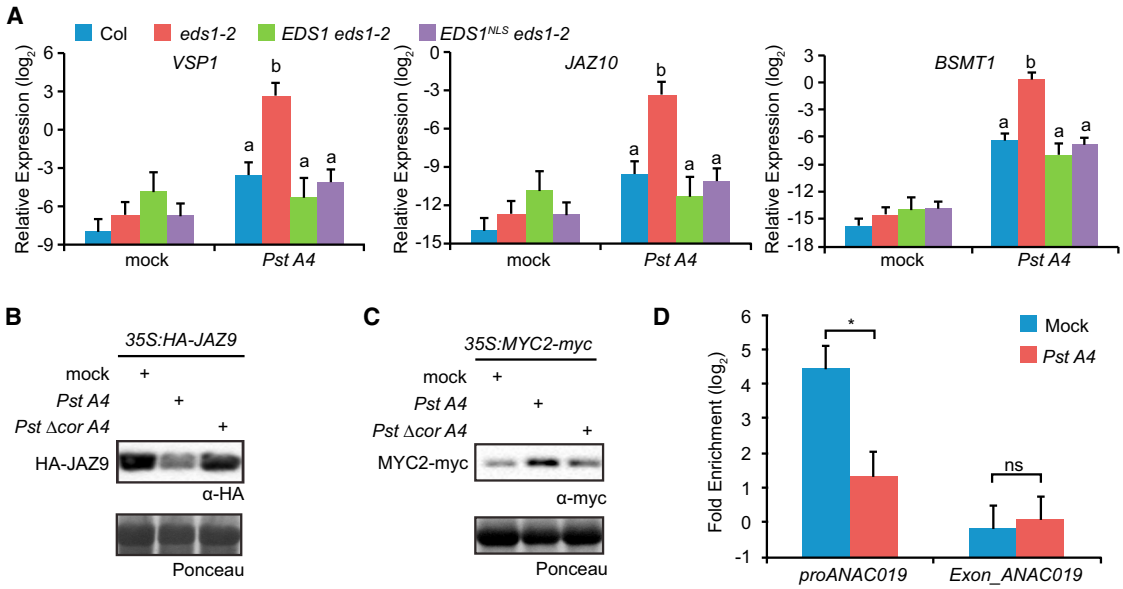

Figure 4. Nuclear EDS1 Interferes with MYC2 Activity.

(A) Expression of *VSP1, JAZ10* and *BSMT1* in Col, *eds1-2*, and transgenic *eds1-2* lines *pEDS1:EDS1-YFP* (*EDS1 eds1-2*) or *pEDS1:EDS1^{NLS}-YFP* (*EDS1^{NLS} eds1-2*) at 24 h after infiltration with the mock control (H_2O) or *Pst AvrRps4* (*Pst A4*) (OD_{600} = 0.002), measured by qRT-PCR. Gene expression was normalized to *AT4G26410.* Bars represent means + SEs calculated from four independent experiments (four biological replicates) using a mixed linear model; different letters indicate statistically significant differences with adjusted *p*-value < 0.01 using the Benjamini–Hochberg method for multiple hypothesis testing.

(B) HA-JAZ9 protein accumulation in transgenic Arabidopsis Col expressing *HA-JAZ9* under the CaMV 35S promoter (*35S:HA-JAZ9*) at 24 hpi with the mock control (H_2O), *Pst AvrRps4* (*Pst A4*), or COR-deficient strain *Pst ⊿cor A4.* Four-week-old plants were infiltrated with bacterial suspensions (OD_{600} = 0.002), and JAZ9 protein was detected in leaf extracts by immunoblotting with α-HA antibody. Ponceau staining of the blot shows equal sample loading.

(C) MYC2-myc protein levels in transgenic Col expressing *MYC2-myc* under the CaMV 35S promoter (*35S:MYC2-myc*) at 24 hpi with mock (H_2O), *Pst A4*, or *Pst ⊿cor A4* treatments as in **(B)**. MYC2 protein was detected in leaf extracts by immunoblotting with α-myc antibody. Ponceau staining of the blot shows equal sample loading.

(D) Analysis of MYC2-myc binding to a target promoter region (containing a G-box motif) of the *ANAC019* gene, measured by ChIP-qPCR in leaf extracts of *35S:MYC2-myc* plants. Binding enrichment was calculated by comparing against a *35S:MYC2-GFP* control line at 24 h after spray inoculation (OD_{600} = 0.2) with the mock control (H_2O) or *Pst A4.* An *ANAC019* exon region was amplified as a negative control (see Methods). Error bars represent means + SEs calculated from three independent experiments (three biological replicates) using a mixed linear model; *, adjusted *p*-value < 0.01 using the Benjamini–Hochberg method for multiple testing; ns, not significant.

in TNL immunity is not simply due to EDS1 interference with MYC2 repression but involves an additional EDS1 mechanism.

TNL/EDS1 Signaling Antagonizes MYC2-Controlled Accumulation of Free SA

Because the above data pointed to EDS1 negative regulation of the MYC2-branch at a different level than the induction of *ICS1* expression, we measured the expression levels of *BSMT1* and *SAGT1* at 24 hpi with *Pst AvrRps4. SAGT1* expression was similar in *eds1-2* and *eds1-2 myc2-3* (Figure 3F). By contrast, *BSMT1* expression was high in *eds1-2* but lower in *eds1-2 myc2-3* (Figure 3G) and in *sid2-1* (Supplemental Figure 3A), suggesting that MYC2 induction of *BSMT1* in *eds1-2* might explain the reduced accumulation of free SA. We therefore constructed an *eds1-2 bsmt1-2* double mutant and measured free and total SA accumulation at 24 hpi with *Pst AvrRps4*. Unlike *eds1-2 myc2-3*, the *eds1-2 bsmt1-2* plants accumulated similar amounts of free and total SA as *eds1-2* (Supplemental Figure 3B). Therefore, MYC2-controlled *BSMT1* expression does not explain the increased free SA in *eds1-2 myc2-3* plants. We concluded that TNL/EDS1 signaling antagonizes MYC2-induced expression of *BSMT1* and other factors that deplete ICS1-generated free SA.

We propose a regulatory circuit in which EDS1 promotes *ICS1* gene expression and counteracts MYC2, thereby bolstering the SA defense sector in TNL immunity (Figure 3H).

Suppression of MYC2 by TNL/EDS1 Occurs in the Nucleus and Does Not Alter JAZ9 Degradation

We investigated the intracellular mechanism by which EDS1 antagonizes the MYC2-branch in TNL immunity. We first tested whether nuclear EDS1 antagonizes MYC2 regulation of genes because nuclear-targeted EDS1-YFP (EDS1^{NLS}-YFP) in Col *eds1-2* plants is sufficient for ETI governed by several TNLs (Garcia et al., 2010; Stuttmann et al., 2016). The EDS1-YFP and EDS1^{NLS}-YFP transgenic lines suppressed MYC2-controlled *VSP1*, *JAZ10* and *BSMT1* expression to the same extent as in wild-type Col at 24 hpi with *Pst AvrRps4* (Figure 4A). These data point to EDS1 pathway interference with MYC2 inside nuclei in RRS1-S/RPS4 immunity.

In unstimulated tissues, MYC2 transcription activity is repressed by association with JAZ proteins in a nuclear repressor complex (Chini et al., 2007; An et al., 2017). JA-Ile or COR binding to SCF^{COI}-JAZ leads to JAZ degradation and release of MYC2

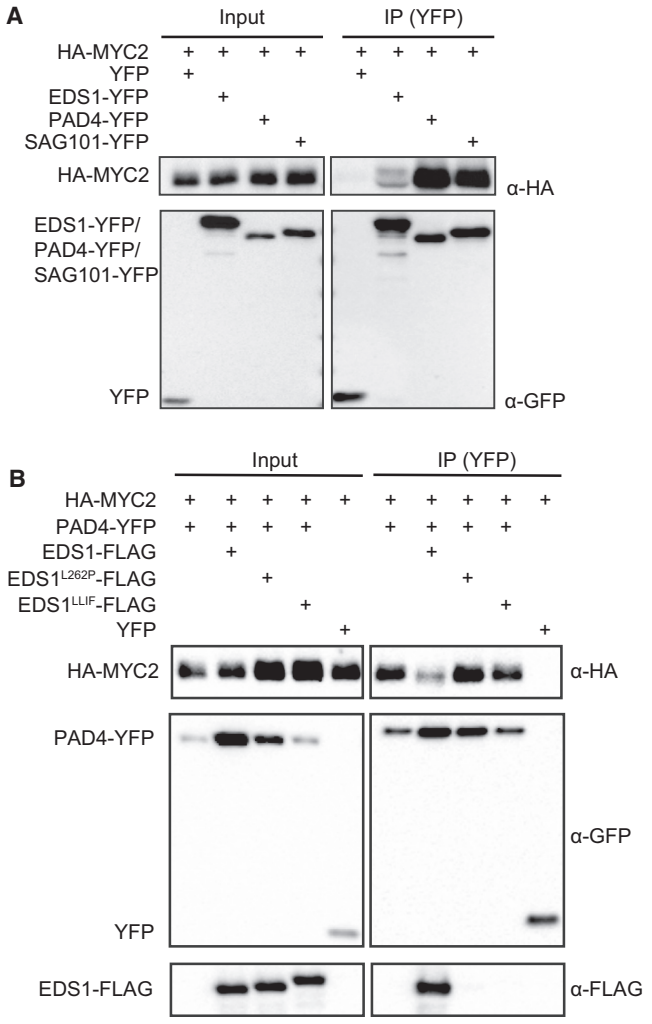

Figure 5. EDS1 Family Proteins Interact with MYC2 *in planta*.

(A) Co-IP analysis of EDS1-YFP, PAD4-YFP or SAG101-YFP with HA-MYC2 at 16 h after transfection of Arabidopsis *eds1-2* protoplasts. Expression of YFP alone served as the control. Proteins in total extracts (Input) and after IP with GFP-trap beads IP (YFP) were detected on immunoblots using α-HA or α-GFP antibody.

(B) Co-IP analysis of PAD4-YFP and HA-MYC2 with and without co-expressed EDS1-FLAG or EDS1-FLAG variants (EDS1^{L262P} and EDS1^{LLIF}) at 16 h after transfection of *eds1-2* protoplasts. IP was performed as in **(A)**, and proteins were detected on immunoblots using α-HA, α-GFP, and α-FLAG antibodies.

Experiments were repeated independently at least twice with similar results.

from repression (Chini et al., 2007; Thines et al., 2007; Sheard et al., 2010; An et al., 2017). We tested whether TNL/EDS1 signaling interferes with COR-induced JAZ degradation by infiltrating an Arabidopsis Col transgenic line expressing HA-tagged JAZ9 driven by the constitutive CaMV *35S* promoter (*35S:HA-JAZ9*) (Yang et al., 2012) with buffer (mock), *Pst AvrRps4*, or *Pst Δcor AvrRps4*. JAZ9 is a direct MYC2 interactor (Fernandez-Calvo et al., 2011). *Pst AvrRps4*, but not *Pst Δcor AvrRps4*, decreased HA-JAZ9 accumulation at 24 hpi compared with mock treatment (Figure 4B). Together, these data suggest that TNL/EDS1 suppression of the MYC2-branch occurs inside the nuclei after or coincident with COR-stimulated JAZ9 degradation.

TNL/EDS1 Signaling Reduces MYC2 Binding to a Target Gene Promoter

MYC2 is regulated by E3 Ubiquitin ligase PUB10-mediated 26S proteasome degradation (Jung et al., 2015), and MYC2 accumulation increases after activation of JA signaling (Zhai et al., 2013). We tested whether triggering of TNL (*RRS1-S/RPS4*) immunity alters MYC2 accumulation in a transgenic Arabidopsis Col line expressing MYC2 with a C-terminal cMyc epitope tag (*35S:MYC2-myc*) (Shin et al., 2012). *Pst AvrRps4*-treated leaves of the *35S:MYC2-myc* line accumulated more MYC2-myc protein at 24 hpi than the mock-treated control or leaves treated with *Pst Δcor AvrRps4* (Figure 4C), consistent with the small but measurable induction of JA-response genes by *Pst AvrRps4* in Col (Figure 2A). Therefore, *Pst AvrRps4* inoculation does not reduce MYC2 accumulation in this transgenic line at 24 hpi.

Using chromatin immunoprecipitation coupled to qPCR (ChIP-qPCR), we tested whether TNL/EDS1 signaling alters MYC2 binding to the promoter of a MYC2-target gene, *ANAC019*, which directly regulates *BSMT1* expression (Zheng et al., 2012). As anticipated, induction of *BSMT1* by *Pst AvrRps4* at 24 hpi was lower in an *anac019 anac055 anac072* triple (*anac*^{3}) mutant compared with Col (Supplemental Figure 4A). We also observed *MYC2*-dependent increased expression of *ANAC019* in *eds1-2* plants at 24 hpi with *Pst AvrRps4* (Supplemental Figure 4B). There was enrichment of MYC2-myc at a MYC2-binding G-box (CACGTG) region in the *ANAC019* promoter in mock-treated *35S:Myc2-myc* leaf samples at 24 h (Figure 4D). The *ANAC019* promoter enrichment of MYC2-myc was lower in *Pst AvrRps4*-treated than in mock-treated samples at 24 hpi (Figure 4D). There were similar background ChIP signals over an *ANAC019* exonic region in all samples (Figure 4D). Accordingly, *Pst AvrRps4*-induced expression of *ANAC019* was dampened to a similar extent in *35S:MYC2-myc* and Col plants, compared with *eds1-2* (Supplemental Figure 4C). These data show that TNL/EDS1 signaling reduces MYC2-chromatin association at the promoter of a MYC2 target gene. We concluded that TNL immunity likely interferes with MYC2 availability or transcriptional activity at MYC2-responsive gene promoters.

EDS1 Family Proteins Interact with MYC2 *in planta*

We investigated whether EDS1 or its direct partners PAD4 and SAG101 associate with MYC2. There was no evidence of direct interaction between EDS1, PAD4, or SAG101 and the MYC2-family proteins MYC2, MYC3, and MYC4 in two different yeast 2-hybrid (Y2H) assays. We then tested for EDS1, PAD4, or SAG101 interactions with MYC2 using transient co-expression assays and immunoprecipitation (IP) in Arabidopsis *eds1-2* protoplasts. First, HA-MYC2 was co-expressed individually with EDS1-YFP, PAD4-YFP, SAG101-YFP or a YFP control. In IP assays using GFP-trap beads, HA-MYC2 immunoprecipitated (IPed) with EDS1-YFP, PAD4-YFP, and SAG101-YFP but not YFP (Figure 5A). The intensity of MYC2-PAD4 and MYC2-SAG101 IP signals was stronger than that of MYC2-EDS1 (Figure 5A, IP), although PAD4 and SAG101 accumulated to lower levels than EDS1 (Figure 5A, input). In an independent set

of IP experiments, FLAG-tagged EDS1, PAD4, SAG101, or YFP were co-expressed individually with HA-MYC2, and anti-FLAG IPs were performed. Here, we observed a similar interaction pattern, in which PAD4-MYC2 and SAG101-MYC2 produced stronger IP signals than EDS1-MYC2 (Supplemental Figure 5A). These data show that PAD4 and SAG101 are each able to interact with MYC2, and EDS1 interacts weakly with MYC2.

EDS1-PAD4 Complexes Reduce PAD4-MYC2 Association

We tested whether PAD4 interaction with MYC2 is affected by the direct association of PAD4 with EDS1 because EDS1 heterodimers with PAD4 or SAG101 signal in TNL immunity (Feys et al., 2005; Wagner et al., 2013). IP experiments with GFP-trap beads were performed in *eds1-2* protoplasts expressing PAD4-YFP/HA-MYC2 with and without co-expressed EDS1-FLAG. Two EDS variants EDS1^{L262P} and EDS1^{LLIF} with mutations in the N-terminal hydrophobic αH-helix , which mediates interaction with PAD4 or SAG101 (Supplemental Figure 5B) (Wagner et al., 2013), were included as controls. Consistent with previous IP experiments (Wagner et al., 2013), PAD4-YFP and SAG101-YFP associated weakly with co-expressed EDS1^{L262P}-FLAG and even more weakly with EDS1^{LLIF}-FLAG (Supplemental Figure 5C and 5D). In accordance with the direct stabilization of PAD4 by EDS1 (Feys et al., 2005), PAD4-YFP accumulation was higher in protoplasts expressing wild-type EDS1-FLAG but moderately and strongly reduced in protoplasts expressing EDS1^{L262P}-FLAG and EDS1^{LLIF}-FLAG, respectively (Supplemental Figure 5C, input). Interaction between PAD4-YFP and HA-MYC2 was weaker in the presence of EDS1-FLAG but not EDS1^{L262P}-FLAG or EDS1^{LLIF}-FLAG (Figure 5B). Therefore, EDS1/PAD4 heterodimers reduce PAD4-MYC2 association.

EDS1-PAD4 Complexes Antagonize MYC2-Regulated Gene Expression

To test further the functional relationship between EDS1 and PAD4 with MYC2 in TNL ETI, we generated two independent homozygous transgenic lines with the PAD4-non-interacting EDS^{LLIF}-YFP variant (#1 and #2) driven by the *EDS1* promoter in the Col *eds1-2* background. These lines accumulated EDS1 protein, although to lower levels than a wild-type EDS1-YFP line (Figure 6A). Both EDS^{LLIF}-YFP lines were susceptible to *Pst* AvrRps4 infection, whereas the control EDS1-YFP line was resistant (Figure 6B). The EDS^{LLIF}-YFP transgenics also failed to antagonize MYC2-promoted expression of *VSP1*, *BSMT1* and *ANAC019* at 24 hpi with *Pst AvrRps4* (Figure 6C and Supplemental Figure 6). These results emphasize the importance of EDS1 association with its partners PAD4 or SAG101 in conferring TNL immunity and antagonizing MYC2.

PAD4 and *SAG101* Suppress the MYC2-Branch in TNL Immunity

The above Arabidopsis EDS1^{LLIF} mutant phenotypes (Figure 6 and Supplemental Figure 6), together with the transient expression and IP data (Figure 5), show that EDS1-PAD4 complexes have a negative effect on PAD4-MYC2 association and the expression of MYC2-controlled genes. We reasoned that this might be because EDS1 sequesters PAD4 from a MYC2-promoting activity, since a PAD4-only activity was reported in Arabidopsis resistance to aphid feeding (Pegadaraju et al., 2007; Louis et al., 2012). We therefore tested the genetic contribution of *PAD4* to *RRS1-S/RPS4* immunity and antagonism of MYC2-controlled gene expression. There was COR-induced susceptibility of *pad4-1* plants to *Pst AvrRps4* (Figure 7A). Also, expression of *VSP1* and *JAZ10* was moderately deregulated in *pad4-1* compared with *eds1-2* and a *pad4-1 sag101-3* double mutant, but not in *sag101-3* plants (Figure 7B), consistent with partial genetic redundancy between *PAD4* and *SAG101* in TNL immunity (Feys et al., 2005; Wagner et al., 2013). These data show that *PAD4* and *SAG101* contribute positively to TNL/*EDS1* pathway suppression of the COR-stimulated MYC2-branch of JA signaling. Hence, PAD4 appears to cooperate with EDS1 in antagonizing rather than promoting MYC2 in TNL ETI.

Finally, we tested for molecular interaction between PAD4 and MYC2 in Arabidopsis plants by crossing the *35S:MYC2-myc* transgenic line with a *pad4-1* mutant complemented by *PAD4-YFP* under control of the native *PAD4* promoter (*pP:PAD4-YFP*). Samples were taken from leaves of *35S:MYC2-myc* and *35S:MYC2-myc/pP:PAD4-YFP pad4-1* plants that were unchallenged or infected with *Pst AvrRps4* at 24 h. MYC2-myc and PAD4-YFP protein levels were higher in input samples after *Pst AvrRps4* treatment (Figure 7C). Interaction between PAD4-YFP and MYC2-myc was detected in TNL-activated but not unchallenged leaf extracts, possibly due to very low accumulation of both proteins in healthy tissues (Figure 7C). These data suggest that there is an interaction between PAD4 and MYC2 during the TNL immune response.

DISCUSSION

Here we provide genetic and molecular evidence that Arabidopsis TNL/EDS1 signaling restricts bacterial pathogen growth inside leaf tissues by interfering with the hub TF MYC2. We show that EDS1/PAD4 complexes mobilize a major portion of the TNL (*RRS1-S/RPS4*) immune response against *Pst AvrRps4* bacteria by antagonizing bacterial COR-stimulated MYC2 transcriptional induction of JA response genes (Figures 1, 2, 3, and 7 and Supplemental Figure 2). One consequence of EDS1/PAD4 negative regulation was lower MYC2-stimulated *BSMT1* expression (Figure 3G and Supplemental Figure 3), which correlated with but did not explain the reduced conversion of free, active SA (Figure 3C and 3D and Supplemental Figure 3B). Independently of antagonizing MYC2, the TNL/EDS1 pathway promoted expression of the SA biosynthetic gene *ICS1*, thereby reinstating SA accumulation and bacterial resistance (Figure 3A, 3B, and 3E). Hence, the data reveal a two-pronged ETI mechanism for steering the host defense network towards SA defenses. Protection of SA-based resistance in ETI makes evolutionary sense for the plant because SA is a vital component of resistance to biotrophic and hemi-biotrophic pathogens (Pieterse et al., 2009) and, as such, is targeted by a range of pathogen effectors in addition to bacterial COR to promote infection (Kazan and Lyons, 2014; Chen et al., 2017; Yang et al., 2017).

EDS1-dependent suppression of the MYC2-responsive genes *VSP1* and *JAZ10* in a TNL autoimmune (*OE-RPS4*) line supplied with exogenous COR (Supplemental Figure 2B) points to

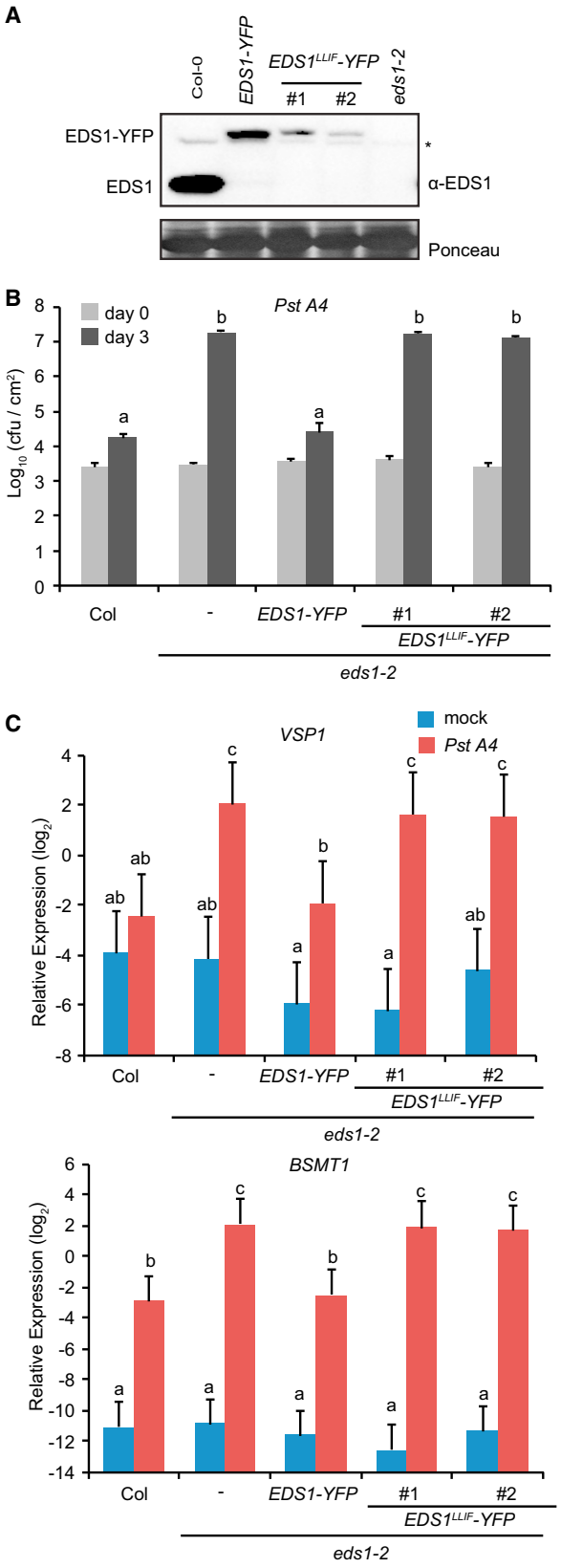

Figure 6. EDS1-PAD4 Association Is Required to Antagonize MYC2.

(A) EDS1 protein accumulation in leaves of 4-week-old transgenic *eds1-2* lines expressing *EDS1-YFP* or *EDS1*^{LLIF}*-YFP* (#1, #2) driven by the *EDS1* promoter was measured on immunoblots probed with α-EDS1 antibody. * indicates a non-specific signal. Ponceau staining of the blot indicates equal loading.

(B) Growth of *Pst AvrRps4* (*Pst A4*) in leaves of the same genotypes as in **(A)** at 0 and 3 dpi. Four-week-old plants were infiltrated with bacterial suspensions (OD_{600} = 0.0002), and bacterial titers were determined. Error bars indicate means + SDs (n = 6 biological replicates in one experiment). Different letters indicate statistical significance ($p < 0.01$) determined by one-way ANOVA with multiple comparison correction by Tukey HSD. Experiments were repeated twice with similar results.

(C) *VSP1* and *BSMT1* expression in leaves of the same genotypes as in **(A)** at 24 hpi with the mock control (H_2O) or *Pst AvrRps4* (*Pst A4*) (OD_{600} = 0.002), measured by qRT-PCR. Gene expression was normalized to *AT4G26410*. Bars represent means + SEs calculated from three independent experiments (three biological replicates) using a mixed linear model; different letters indicate statistically significant differences with adjusted *p*-value < 0.01 using the Benjamini–Hochberg method for multiple hypothesis testing.

antagonism of MYC2 transcription activity after COR has activated signaling via SCF^{COI1}-JAZ receptors in host cells. Moreover, interference with COR-induced expression of MYC2-branch genes by nuclear-targeted EDS1^{NLS}-YFP (Figure 4A) suggests that EDS1 antagonizes MYC2 in the nucleus rather than impeding MYC2 access to nuclei where it normally localizes and functions (Kazan and Manners, 2013; An et al., 2017). The antagonism of MYC2 in TNL ETI reduces MYC2 binding to a responsive promoter (*pANAC019*) (Figure 4D). Whether this occurs at the chromatin where MYC2 becomes activated (An et al., 2017) is not clear. Because MYC2 is a transcriptional hub, the effects of ETI suppression of MYC2 likely ramify to other MYC2-controlled pathways, such as those involved in abiotic stress signaling and secondary metabolite production (Kazan and Manners, 2013; Frerigmann et al., 2014).

We detected a substantial reduction (>1.0 $\log_{10}$) in *Pst AvrRps4* growth in *eds1 coi1-41* and *eds1-2 myc2-3* leaves (Figures 1B, 3A, and 3B), and found a major *MYC2* contribution to *BSMT1* expression and dampening of free SA accumulation in TNL (*RRS1-S/RPS4*) resistance after bacterial infiltration (Figure 3C, 3D, and 3G), indicative of a post-stomatal mechanism. Besides promoting *ICS1* expression, EDS1/PAD4 buffer the SA defense sector against pathogen or genetic perturbations. Thus, some SA-responsive gene expression and bacterial resistance is preserved in an *ics1* mutant (Cui et al., 2017). An *ICS1*-independent TNL branch promotes resistance via EDS1/PAD4 interference with bacterial COR-stimulated MYC2 of target genes because dampening of MYC2-induced *VSP1*, *JAZ10* and *BSMT1* expression did not require *ICS1* (Figure 2D, Supplemental Figures 2B and 3). Zheng et al. (2012) reported that MYC2 negatively regulates basal *ICS1* gene expression. Therefore, we reasoned that TNL/EDS1 antagonism of MYC2 might explain stimulation of *ICS1* expression in *RRS1-S/RPS4* immunity. However, *ICS1* expression was not significantly higher in untreated *myc2-3* leaves relative to Col in our experiments (Figure 3E). Moreover, *ICS1* induction in *Pst AvrRps4*-treated *myc2-3* plants still required *EDS1* (Figure 3E), indicative of an additional *EDS1*-controlled mechanism(s) driving *ICS1* expression in TNL ETI (Figure 3H).

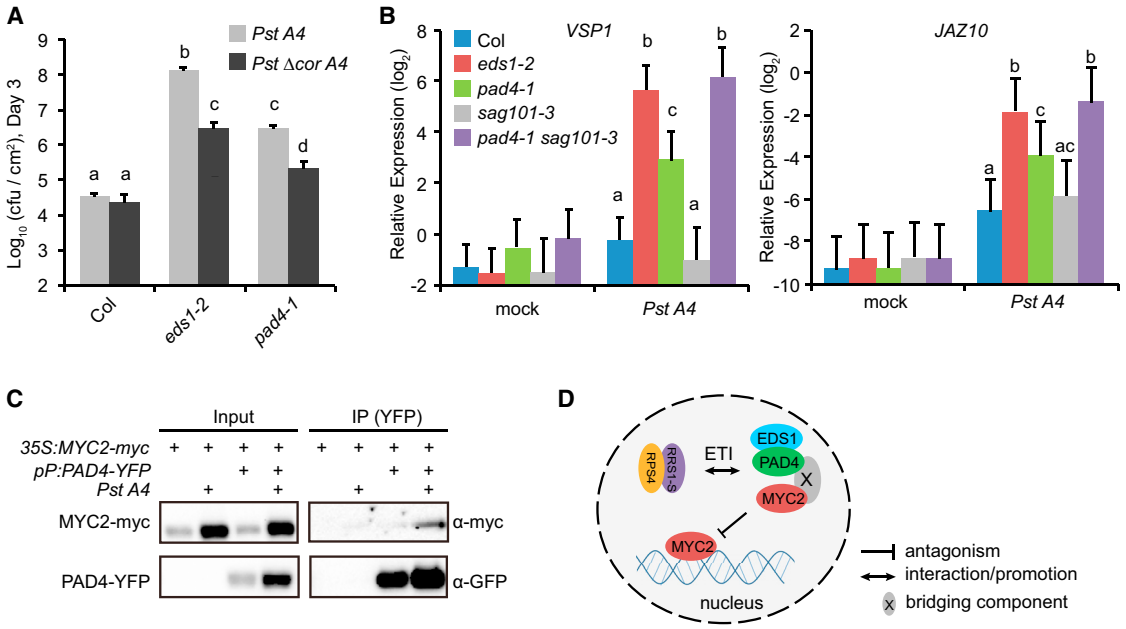

Figure 7. *PAD4* and *SAG101* Suppress the MYC2-Branch in TNL Immunity.

(A) Growth of *Pst AvrRps4* (*Pst A4*) and COR deficient strain *Pst ΔcorA4* in leaves of Col, *eds1-2* and *pad4-1*. Four-week-old plants were infiltrated with bacterial suspensions (OD_{600} = 0.0002), and bacterial titers were determined at 3 dpi. Error bars indicate means + SDs (n = 4 biological replicates in one experiment). Different letters indicate statistical significance ($p < 0.01$) determined by one-way ANOVA with multiple comparison correction by Tukey HSD. Experiments were repeated twice with similar results.

(B) Expression of *VSP1* and *JAZ10* in Col, *eds1-2, pad4-1, sag101*, and *pad4-1 sag101-3* plants at 24 hpi with the mock control (H_2O) or *Pst A4,* measured by qRT-PCR. Four-week-old plants were infiltrated with *Pst A4* (OD_{600} = 0.002). Gene expression was normalized to *AT4G26410.* Bars represent means + SEs calculated from four independent experiments (four biological replicates) using a mixed linear model; different letters indicate statistically significant differences with adjusted *p*-value < 0.01 using the Benjamini–Hochberg method for multiple hypothesis testing.

(C) Co-IP analysis of PAD4 with MYC2 was performed on 2-week-old seedlings of a transgenic *35S:MYC2-myc/pP:PAD4-YFP pad4-1* line that were untreated or inoculated at 24 hpi with *Pst AvrRps4* (*Pst* A4). Proteins in total leaf extracts (Input) and after IP with GFP-trap beads (YFP) were detected on immunoblots using α-myc and α-GFP antibodies, as shown. Experiments were repeated twice with similar results.

(D) A schematic diagram showing EDS1-PAD4 inhibition of MYC2 in RRS1-S/RPS4 (TNL) ETI. PAD4 likely associates with MYC2 via a bridging component (depicted as X) because direct interaction has not been established. In RRS1-S/RPS4 ETI, the EDS1-PAD4 heterodimer has MYC2-suppressing activity, leading to reduced MYC2 availability at target gene promoters.

Activation of TNL/EDS1 immunity also antagonized the COR-stimulated ERF-branch of JA signaling, indicated by higher expression of ORA59/ERF1-controlled *PDF1.2* in *eds1-2* than in Col (Figure 2D). We presume that antagonism of this COR branch occurs via EDS1 promotion of *ICS1*-generated SA because it was *ICS1*-dependent (Figure 2D). COR/JA-stimulated MYC2 imposes negative control on the ERF-branch through direct repression of *ERF1* and *ORA59*, although the precise mechanism of MYC2 repression remains unclear (Kazan and Manners, 2013). ICS1-generated SA reduces *PDF1.2* expression through proteasome-mediated degradation of ORA59, independently of COI1/JAZ receptor functions (Van der Does et al., 2013). These intricate negative regulatory circuits enable the plant to prioritize its response against conflicting stresses. Our pathway analysis suggests that TNL ETI signaling steers hormone pathway balance away from the two major JA-signaling branches in a different way by (i) interfering with MYC2-regulated gene expression and (ii) stimulating *ICS1* expression (Figure 3H).

While reciprocal antagonism between SA and JA pathways is important for fine-control of plant biotic stress signaling, instances of SA-JA synergy that depend on the timing and flux through these hormone systems have been reported (Mur et al., 2006; Mine et al., 2017b). Early perturbation of SA-JA antagonism (at 4 h) in Arabidopsis ETI is conferred by the CNL receptor RPS2, and a positive contribution of JA-signaling to *RPS2* resistance and cell death has been described (Liu et al., 2016). It is possible that SA-JA cooperation occurs early in the Col TNL (*RRS1-S/RPS4*) immune response because MYC2 protein accumulated (Figures 4C and 7C) and JA-signaling and response genes were induced in wild-type Col at 6, 8 and 24 hpi with *Pst AvrRps4* (Figure 2A and 2D) (Bartsch et al., 2006). Nevertheless, induction of MYC2-controlled JA response genes was restricted in an *RRS1-S/RPS4*- and *EDS1*-dependent manner (Figure 2A, 2C, and 2D), indicating a mainly antagonistic relationship and emphasizing the importance of prioritizing SA over JA pathways in the TNL immune response.

Our genetic and molecular data support a mode of EDS1/PAD4 interference with MYC2 that involves PAD4 interaction with MYC2 (Figures 5 and 7). This is likely to be via a bridging component(s) (Figure 7D) since we did not observe direct protein interactions in Y2H assays. In our IP analysis, PAD4 association with MYC2 was limited by direct EDS1 binding to PAD4 (Figure 5), suggesting a role of EDS1 in modulating PAD4-MYC2

interaction and function. Because dampening of MYC2 activity is mediated by EDS1 together with PAD4 or SAG101 in a complex (Figures 6 and 7), we propose that TNL effector recognition confers on the EDS1 heterodimer a MYC2-suppressing activity. This activity reduces MYC2 availability at the promoters of target genes involved in mobilizing SA-antagonizing JA and potentially numerous other MYC2-controlled pathways (Figure 7D). Reduced steady-state PAD4-MYC2 interaction in the presence of EDS1 might reflect a MYC2-inhibiting activity, accompanied by turnover or release of EDS1/PAD4 from a MYC2-containing complex. Phosphorylation and poly-ubiquitination have been shown to regulate MYC2 protein turnover and transcriptional activity in JA signaling (Zhai et al., 2013; Jung et al., 2015). Because we observed increased MYC2 accumulation in TNL-triggered leaf extracts (Figures 4C and 7C), we think it likely that EDS1/PAD4 alter the relationship between MYC2 and other factors to regulate MYC2 outputs in TNL ETI. Functional connectivity between MYC2 and other TFs, as well as subunits of the MEDIATOR transcriptional processing complex and histone acetyltransferase 1, present opportunities for disturbing MYC2 functions at gene promoters (Kazan and Manners, 2013; Frerigmann et al., 2014; An et al., 2017).

This analysis shows that a portion of total *EDS1/PAD4* activity in *RRS1-S/RPS4* ETI can be attributed to nuclear antagonism of COR-stimulated MYC2 and a reinstatement of SA resistance, as measured by *Pst AvrRps4* growth (Figure 3A and 3B). Future experiments will address the molecular mechanism of interference. Stripping away this immunity sector in *eds1 myc2* or *eds1 coi1* mutants also provides material to explore the nature of the remaining factors involved in TNL/EDS1-controlled resistance.

METHODS

Plant Materials, Growth Conditions and Pathogen Strains

Arabidopsis accession Col was used in all experiments. The *eds1-2* (Bartsch et al., 2006), *pad4-1* (Jirage et al., 1999), *dde2-2* (Tsuda et al., 2009), *rrs1a/b* (*rrs1-3/rrs1b*) (Saucet et al., 2015), *coi1-1* (Feys et al., 1994), *sid2-1* (Wildermuth et al., 2001), *eds1-2 sid2-1* (Cui et al., 2017), *myc2-3* (Shin et al., 2012), *bsmt1-2* (Attaran et al., 2009), and *anac019 anac055 anac072* (Zheng et al., 2012) mutants are published. *Sag101-3* is a T-DNA insertion from the GABI-kat population (line ID: 476E10). *Pad4-1 sag101-3, eds1-2 dde2-2, eds1-2 bsmt1-2* and *eds1-2 myc2-3* double mutants were generated by crossing the corresponding single mutants with *eds1-2*. An *eds1-2 myc2-3 sid2-1* triple mutant was generated by crossing *eds1-2 myc2-3* with *eds1-2 sid2-1*. Transgenic lines *35S:HA-JAZ9* in Col (Yang et al., 2012), *35S:MYC2-myc* in Col (Shin et al., 2012), *35S:MYC2-GFP* (Mine et al., 2017b), and *OE-RPS4* Col and *OE-RPS4 eds1-2* (Heidrich et al., 2013) were characterized previously. *OE-RPS4 sid2-1* lines were generated by crossing *OE-RPS4* Col with *sid2-1*. A *35S:MYC2-myc/pP:PAD4-YFP pad4-1* line was generated by crossing *35S:MYC2-myc* with a *PAD4* promoter-driven *pP:PAD4-YFP pad4-1* line. *EDS1-YFP eds1-2* transgenic lines were generated as previously described (Garcia et al., 2010). *Pseudomonas syringe* pv. *tomato* (*Pst*) strain DC3000 *AvrRps4* and *Pst ΔCor AvrRps4* were previously described (Cui et al., 2017). Seeds were germinated in soil, and plants were grown under a 10 h light regime (150-200 ìE/m^{2}s) at 22°C and 60% relative humidity.

Pathogen Infection Assays

For mutant screening, 2-week-old seedlings were sprayed with *Pst AvrRps4* bacteria (OD_{600} = 0.2) in H_2O plus 0.03% silwet L-77, and the seedlings kept under covers for 6 d at 22°C. For bacterial growth assays, *Pst AvrRps4* or *Pst ΔCor AvrRps4* (OD_{600} = 0.0002) in H_2O were hand-infiltrated into leaves of 4-week-old plants, and bacterial titers were measured as previously described (Feys et al., 2005). Statistical analysis of bacterial growth data from 4 - 6 biological replicates (as indicated in the figure legends) was done by one-way ANOVA with multiple comparison correction using Tukey HSD. For gene and protein expression assays, leaves from 4-week-old plants were hand-infiltrated with bacteria (OD_{600} = 0.002), and samples were taken at the indicated time points.

Root Growth Inhibition Assays

Arabidopsis seeds were surface-sterilized, stratified and germinated on half-strength Murashige and Skoog (MS) media for 3 d, then transferred to square plates standing vertically with half-strength MS media containing COR or DMSO at indicated concentrations for 10–12 d before imaging roots. Seedlings were grown under a 12 h light regime (100 ìE/m^{2}s) at 22°C. Root lengths were measured using ImageJ software (https://imagej.nih.gov/ij/).

Plasmid Constructs

Entry vectors pENTR-*genomicEDS1*, pENTR-*PAD4* and pENTR-*SAG101* were previously described (Wagner et al., 2013). The MYC2 open reading frame without a stop codon was PCR-amplified from Col cDNA and cloned into Gateway pENTR-D/TOPO by TOPO cloning (Invitrogen). The pENTR-*genomicEDS1*^{L262P} and pENTR-*genomicEDS1*^{LLIF} constructs were generated by site-directed mutagenesis PCR using pENTR-*genomicEDS1* as template. *YFP* without a stop codon was cloned into pENTR-D/TOPO. The pENTR clones were recombined into various Gateway destination vectors using Gateway LR reactions (Invitrogen) to fuse ORFs to N-terminal HA or C-terminal YFP, FLAG or 6xmyc epitopes under the control of the *35S* promoter, as indicated.

Generation of Arabidopsis Transgenic Plants

Previously generated entry clones pENTR-*pPAD4:PAD4* (Wagner et al., 2013) and the newly made entry clones pENTR-*pEDS1:gEDS1* and pENTR-*pEDS1:gEDS1*^{LLIF} were recombined with the binary destination vector *pXCG-mYFP* to obtain a construct with *PAD4-YFP* expression driven by the *PAD4* promoter (*pP:PAD4-YFP*) and constructs with *gEDS1-YFP* or *gEDS1*^{LLIF}*-YFP* expression driven by the *EDS1* promoter. Binary expression vectors were transformed by *Agrobacterium*-mediated floral dipping into Arabidopsis *pad4-1* or *eds1-2* plants, as indicated.

qRT-PCR and Statistical Analysis

Total leaf RNA from six plants was extracted using a Plant RNA kit (Biobudget) as one biological replicate. 1 μg total RNA was used for cDNA synthesis (Thermo Fisher Scientific), and qRT-PCR analysis was done on a CFX Connect machine (Biorad). Expression of the test gene was normalized to *AT4G26410* (Cui et al., 2017). Statistical analysis of qRT-PCR data from three biological replicates (as three independent experiments) was done using the lme4 package in the R environment, as previously described (Tsuda et al., 2009; Mine et al., 2017a). Relative Ct values were generated and the following models were fitted to the data: $Ct_{gyr} = GY_{gy}+R_r+e_{gyr}$ and $Ct_{ytr} = YT_{yt}+R_r+e_{ytr}$, where GY is genotype:treatment interaction, YT is the treatment:time interaction, and the random factors R and e are biological replicate and residual, respectively. The mean estimates of the fixed effects were used as modeled relative Ct values, visualized as $\log_2$ expression values, and compared using two-tailed t-tests. For the t-tests, standard errors were calculated using variance and covariance values obtained from the linear model fitting. The Benjamini-Hochberg method was used to correct for multiple hypothesis testing in pairwise comparisons of the mean estimates shown in the figures.

Chromatin Immunoprecipitation (ChIP)

For MYC2-myc ChIP, 2-week-old seedlings were spray-inoculated with *Pst AvrRps4* (OD600 = 0.2) in H_2O plus 0.02% silwet L-77 or with a mock treatment (H_2O plus 0.02% silwet L-77) and harvested at 24 h.

ChIP experiments were performed as previously described (Reimer and Turck, 2010) using α-myc antibody (ab9132, Abcam), and samples were analyzed by qPCR. Primers in the promoter (from -1026 to -896) or the exon (from 740 to 857) used for qPCR are listed in Supplemental Table 3. Relative Ct values were compared to input samples to determine IP enrichment, and then fold enrichment was calculated as the ratio between IP enrichment in *35S:MYC2* and control *35S:MYC2-GFP* plants. For statistical analysis using R, the following model was fitted to the data from three biological repeats (three independent experiments): $Ct_{gyr} = GY_{gy}+R_r+e_{gyr}$, where GY is the primer:treatment interaction and random factors R and e are biological replicate and residual, respectively. Mean estimates of the fixed effects were used to model relative $\log_2$ fold enrichment values and were compared using two-tailed t-tests.

Transient Expression in Arabidopsis Mesophyll Protoplasts

Protoplast preparations from 4-week-old *eds1-2* plants and transfections were done according to (Yoo et al., 2007). After transfection, protoplasts were incubated at room temperature under weak light (1.5 ìE/m^2s) for 16 h, and protein extracts were prepared for immunoblotting and IP assays.

Protein Extraction, Immunoprecipitation and Immunoblotting

Total leaf or protoplast proteins were processed in extraction buffer (50 mM Tris pH7.5, 150 mM NaCl, 10% (v/v) glycerol, 2 mM EDTA, 5 mM DTT, protease inhibitor (Roche, 1 tablet per 50 mL), 0.1% Triton). Lysates were centrifuged for 15 min at 14 000 rpm at 4°C. Aliquots of supernatants were used as input samples. Immunoprecipitations were conducted by incubating supernatants with 20 μl GFP-Trap or anti-FLAG-coupled beads (Chromotek) in 1.5 mL tubes for 2 h at 4°C. Beads were collected by centrifugation and washed four times in extraction buffer. Beads were then heated in 2×Laemmli loading buffer, and proteins were separated by SDS-PAGE and analyzed by immunoblotting. Antibodies used were α-GFP (Sigma Aldrich, 11814460001), α-HA (Sigma Aldrich, 11867423001), α-FLAG (Sigma Aldrich, F3165), and α-cMyc (Sigma Aldrich, M4439). Secondary antibodies were coupled to Horseradish Peroxidase (Santa Cruz Biotechnology, Dallas).

Selection of JA-Induced Genes Using Genevestigator

Genes highly induced in *eds1-2* infiltrated with *Pst AvrRps4* compared with the mock treatment in a microarray data set (E-MEXP-546) were selected and used as input genes in the Genevestigator Tool (https://genevestigator.com/gv/). Microarray data sets from JA or Me-JA studies were used to select JA-induced genes using the Perturbations tool in Genevestigator. A heatmap was generated with the software CLUSTER using uncentered Pearson correlations and complete linkage clustering and was visualized using TREEVIEW software (Eisen et al., 1998).

Total and Free SA Quantitation

Total and free SA was quantified in leaf tissues as previously described (Straus et al., 2010).

SUPPLEMENTAL INFORMATION

Supplemental Information is available at *Molecular Plant Online*.

FUNDING

This work was funded by The Max Planck Society, an Alexander von Humboldt Foundation postdoctoral fellowship, and the National Nature Science Foundation of China (Grant 31770277) (HC), a Chinese Scholarship Council PhD fellowship (CSC) (JQ) and Deutsche Forschungsgemeinschaft SFB 670 grant (JEP, DB).

AUTHOR CONTRIBUTIONS

HC and JEP designed and supervised the research; HC and JQ carried out the *eds1-2* mutant screen and characterization, qRT-PCR and IP experiments, and pathogen infection assays; HC and YZ did the MYC2 ChIP-qPCR analysis; DB performed protein structure and SA analyses; JB generated and characterized EDS1 transgenic lines; CZ helped characterizing *bsmt1* mutant lines. JEP and HC wrote the manuscript with contributions from JQ.

ACKNOWLEDGMENTS

We thank Sheng Yang He for sharing the *35S:HA-JAZ9* overexpression lines, Seth Davis for providing the *35S:MYC2-myc* lines, Alain Goossens for doing Y2H assays, and Paul Schulze-Lefert, Kenichi Tsuda and Takaki Maekawa for helpful discussions. No conflict of interest declared.

Received: December 19, 2017
Revised: April 26, 2018
Accepted: May 21, 2018
Published: May 26, 2018

REFERENCES

An, C., Li, L., Zhai, Q., You, Y., Deng, L., Wu, F., Chen, R., Jiang, H., Wang, H., Chen, Q., et al. (2017). Mediator subunit MED25 links the jasmonate receptor to transcriptionally active chromatin. Proc. Natl. Acad. Sci. USA **114**:E8930–E8939.

Attaran, E., Zeier, T.E., Griebel, T., and Zeier, J. (2009). Methyl salicylate production and jasmonate signaling are not essential for systemic acquired resistance in *Arabidopsis*. Plant Cell **21**:954–971.

Bartsch, M., Gobbato, E., Bednarek, P., Debey, S., Schultze, J.L., Bautor, J., and Parker, J.E. (2006). Salicylic acid-independent ENHANCED DISEASE SUSCEPTIBILITY1 signaling in *Arabidopsis* immunity and cell death is regulated by the monooxygenase FMO1 and the Nudix hydrolase NUDT7. Plant Cell **18**:1038–1051.

Bhattacharjee, S., Halane, M.K., Kim, S.H., and Gassmann, W. (2011). Pathogen effectors target *Arabidopsis* EDS1 and alter its interactions with immune regulators. Science **334**:1405–1408.

Brooks, D.M., Bender, C.L., and Kunkel, B.N. (2005). The *Pseudomonas syringae* phytotoxin coronatine promotes virulence by overcoming salicylic acid-dependent defences in *Arabidopsis thaliana*. Mol. Plant Pathol. **6**:629–639.

Chen, H., Chen, J., Li, M., Chang, M., Xu, K., Shang, Z., Zhao, Y., Palmer, I., Zhang, Y., McGill, J., et al. (2017). A bacterial type III effector targets the master regulator of salicylic acid signaling, NPR1, to subvert plant immunity. Cell Host Microbe **22**:777–788.e7.

Cheng, Y.T., Germain, H., Wiermer, M., Bi, D., Xu, F., Garcia, A.V., Wirthmueller, L., Despres, C., Parker, J.E., Zhang, Y., et al. (2009). Nuclear pore complex component MOS7/Nup88 is required for innate immunity and nuclear accumulation of defense regulators in *Arabidopsis*. Plant Cell **21**:2503–2516.

Chini, A., Fonseca, S., Fernandez, G., Adie, B., Chico, J.M., Lorenzo, O., Garcia-Casado, G., Lopez-Vidriero, I., Lozano, F.M., Ponce, M.R., et al. (2007). The JAZ family of repressors is the missing link in jasmonate signalling. Nature **448**:666–671.

Cui, H., Tsuda, K., and Parker, J.E. (2015). Effector-triggered immunity: from pathogen perception to robust defense. Annu. Rev. Plant Biol. **66**:487–511.

Cui, H., Gobbato, E., Kracher, B., Qiu, J., Bautor, J., and Parker, J.E. (2017). A core function of EDS1 with PAD4 is to protect the salicylic acid defense sector in *Arabidopsis* immunity. New Phytol. **213**:1802–1817.

Eisen, M.B., Spellman, P.T., Brown, P.O., and Botstein, D. (1998). Cluster analysis and display of genome-wide expression patterns. Proc. Natl. Acad. Sci. USA **95**:14863–14868.

Fernandez-Calvo, P., Chini, A., Fernandez-Barbero, G., Chico, J.M., Gimenez-Ibanez, S., Geerinck, J., Eeckhout, D., Schweizer, F., Godoy, M., Franco-Zorrilla, J.M., et al. (2011). The *Arabidopsis* bHLH transcription factors MYC3 and MYC4 are targets of JAZ repressors and act additively with MYC2 in the activation of jasmonate responses. Plant Cell **23**:701–715.

Feys, B., Benedetti, C.E., Penfold, C.N., and Turner, J.G. (1994). *Arabidopsis* mutants selected for resistance to the phytotoxin coronatine are male sterile, insensitive to methyl jasmonate, and resistant to a bacterial pathogen. Plant Cell **6**:751–759.

Feys, B.J., Wiermer, M., Bhat, R.A., Moisan, L.J., Medina-Escobar, N., Neu, C., Cabral, A., and Parker, J.E. (2005). *Arabidopsis* SENESCENCE-ASSOCIATED GENE101 stabilizes and signals within an ENHANCED DISEASE SUSCEPTIBILITY1 complex in plant innate immunity. Plant Cell **17**:2601–2613.

Frerigmann, H., Berger, B., and Gigolashvili, T. (2014). bHLH05 is an interaction partner of MYB51 and a novel regulator of glucosinolate biosynthesis in *Arabidopsis*. Plant Physiol. **166**:349–369.

Fu, Z.Q., and Dong, X. (2013). Systemic acquired resistance: turning local infection into global defense. Annu. Rev. Plant Biol. **64**:839–863.

Garcia, A.V., Blanvillain-Baufume, S., Huibers, R.P., Wiermer, M., Li, G., Gobbato, E., Rietz, S., and Parker, J.E. (2010). Balanced nuclear and cytoplasmic activities of EDS1 are required for a complete plant innate immune response. PLoS Pathog. **6**:e1000970.

Gu, Y., Zebell, S.G., Liang, Z., Wang, S., Kang, B.H., and Dong, X. (2016). Nuclear pore permeabilization is a convergent signaling event in effector-triggered immunity. Cell **166**:1526–1538.e11.

Heidrich, K., Wirthmueller, L., Tasset, C., Pouzet, C., Deslandes, L., and Parker, J.E. (2011). *Arabidopsis* EDS1 connects pathogen effector recognition to cell compartment-specific immune responses. Science **334**:1401–1404.

Heidrich, K., Tsuda, K., Blanvillain-Baufume, S., Wirthmueller, L., Bautor, J., and Parker, J.E. (2013). *Arabidopsis* TNL-WRKY domain receptor RRS1 contributes to temperature-conditioned RPS4 auto-immunity. Front. Plant Sci. **4**:403.

Hillmer, R.A., Tsuda, K., Rallapalli, G., Asai, S., Truman, W., Papke, M.D., Sakakibara, H., Jones, J.D.G., Myers, C.L., and Katagiri, F. (2017). The highly buffered *Arabidopsis* immune signaling network conceals the functions of its components. PLoS Genet. **13**:e1006639.

Huh, S.U., Cevik, V., Ding, P., Duxbury, Z., Ma, Y., Tomlinson, L., Sarris, P.F., and Jones, J.D.G. (2017). Protein-protein interactions in the RPS4/RRS1 immune receptor complex. PLoS Pathog. **13**:e1006376.

Jacob, F., Kracher, B., Mine, A., Seyfferth, C., Blanvillain-Baufume, S., Parker, J.E., Tsuda, K., Schulze-Lefert, P., and Maekawa, T. (2018). A dominant-interfering camta3 mutation compromises primary transcriptional outputs mediated by both cell surface and intracellular immune receptors in *Arabidopsis thaliana*. New Phytol. **217**:1667–1680.

Jirage, D., Tootle, T.L., Reuber, T.L., Frost, L.N., Feys, B.J., Parker, J.E., Ausubel, F.M., and Glazebrook, J. (1999). *Arabidopsis thaliana* PAD4 encodes a lipase-like gene that is important for salicylic acid signaling. Proc. Natl. Acad. Sci. USA **96**:13583–13588.

Jones, J.D., Vance, R.E., and Dangl, J.L. (2016). Intracellular innate immune surveillance devices in plants and animals. Science **354**.

Jung, C., Zhao, P., Seo, J.S., Mitsuda, N., Deng, S., and Chua, N.H. (2015). PLANT U-BOX PROTEIN10 regulates MYC2 stability in *Arabidopsis*. Plant Cell **27**:2016–2031.

Kazan, K., and Lyons, R. (2014). Intervention of phytohormone pathways by pathogen effectors. Plant Cell **26**:2285–2309.

Kazan, K., and Manners, J.M. (2013). MYC2: the master in action. Mol. Plant **6**:686–703.

Kim, T.H., Kunz, H.H., Bhattacharjee, S., Hauser, F., Park, J., Engineer, C., Liu, A., Ha, T., Parker, J.E., Gassmann, W., et al. (2012). Natural variation in small molecule-induced TIR-NB-LRR signaling induces root growth arrest via EDS1- and PAD4-complexed R protein VICTR in *Arabidopsis*. Plant Cell **24**:5177–5192.

Kim, S.H., Son, G.H., Bhattacharjee, S., Kim, H.J., Nam, J.C., Nguyen, P.D., Hong, J.C., and Gassmann, W. (2014). The *Arabidopsis* immune adaptor SRFR1 interacts with TCP transcription factors that redundantly contribute to effector-triggered immunity. Plant J. **78**:978–989.

Liu, L., Sonbol, F.M., Huot, B., Gu, Y., Withers, J., Mwimba, M., Yao, J., He, S.Y., and Dong, X. (2016). Salicylic acid receptors activate jasmonic acid signalling through a non-canonical pathway to promote effector-triggered immunity. Nat. Commun. **7**:13099.

Louis, J., Gobbato, E., Mondal, H.A., Feys, B.J., Parker, J.E., and Shah, J. (2012). Discrimination of *Arabidopsis* PAD4 activities in defense against green peach aphid and pathogens. Plant Physiol. **158**:1860–1872.

Maekawa, T., Kufer, T.A., and Schulze-Lefert, P. (2011). NLR functions in plant and animal immune systems: so far and yet so close. Nat. Immunol. **12**:817–826.

Melotto, M., Underwood, W., Koczan, J., Nomura, K., and He, S.Y. (2006). Plant stomata function in innate immunity against bacterial invasion. Cell **126**:969–980.

Mine, A., Berens, M.L., Nobori, T., Anver, S., Fukumoto, K., Winkelmuller, T.M., Takeda, A., Becker, D., and Tsuda, K. (2017a). Pathogen exploitation of an abscisic acid- and jasmonate-inducible MAPK phosphatase and its interception by *Arabidopsis* immunity. Proc. Natl. Acad. Sci. USA **114**:7456–7461.

Mine, A., Nobori, T., Salazar-Rondon, M.C., Winkelmuller, T.M., Anver, S., Becker, D., and Tsuda, K. (2017b). An incoherent feed-forward loop mediates robustness and tunability in a plant immune network. EMBO Rep. **18**:464–476.

Mur, L.A., Kenton, P., Atzorn, R., Miersch, O., and Wasternack, C. (2006). The outcomes of concentration-specific interactions between salicylate and jasmonate signaling include synergy, antagonism, and oxidative stress leading to cell death. Plant Physiol. **140**:249–262.

Narusaka, M., Toyoda, K., Shiraishi, T., Iuchi, S., Takano, Y., Shirasu, K., and Narusaka, Y. (2016). Leucine zipper motif in RRS1 is crucial for the regulation of *Arabidopsis* dual resistance protein complex RPS4/RRS1. Sci. Rep. **6**:18702.

Nobori, T., Velasquez, A.C., Wu, J., Kvitko, B.H., Kremer, J.M., Wang, Y., He, S.Y., and Tsuda, K. (2018). Transcriptome landscape of a bacterial pathogen under plant immunity. Proc. Natl. Acad. Sci. USA **115**:E3055–E3064.

Padmanabhan, M.S., Ma, S., Burch-Smith, T.M., Czymmek, K., Huijser, P., and Dinesh-Kumar, S.P. (2013). Novel positive regulatory role for the SPL6 transcription factor in the N TIR-NB-LRR receptor-mediated plant innate immunity. PLoS Pathog. **9**:e1003235.

Pegadaraju, V., Louis, J., Singh, V., Reese, J.C., Bautor, J., Feys, B.J., Cook, G., Parker, J.E., and Shah, J. (2007). Phloem-based resistance to green peach aphid is controlled by *Arabidopsis* PHYTOALEXIN DEFICIENT4 without its signaling partner ENHANCED DISEASE SUSCEPTIBILITY1. Plant J. **52**:332–341.

Pieterse, C.M., Leon-Reyes, A., Van der Ent, S., and Van Wees, S.C. (2009). Networking by small-molecule hormones in plant immunity. Nat. Chem. Biol. **5**:308–316.

Reimer, J.J., and Turck, F. (2010). Genome-wide mapping of protein-DNA interaction by chromatin immunoprecipitation and DNA microarray hybridization (ChIP-chip). Part A: ChIP-chip molecular methods. Methods Mol. Biol. **631**:139–160.

Saucet, S.B., Ma, Y., Sarris, P.F., Furzer, O.J., Sohn, K.H., and Jones, J.D. (2015). Two linked pairs of *Arabidopsis* TNL resistance genes independently confer recognition of bacterial effector AvrRps4. Nat. Commun. **6**:6338.

Sheard, L.B., Tan, X., Mao, H., Withers, J., Ben-Nissan, G., Hinds, T.R., Kobayashi, Y., Hsu, F.F., Sharon, M., Browse, J., et al. (2010). Jasmonate perception by inositol-phosphate-potentiated COI1-JAZ co-receptor. Nature **468**:400–405.

Shin, J., Heidrich, K., Sanchez-Villarreal, A., Parker, J.E., and Davis, S.J. (2012). TIME FOR COFFEE represses accumulation of the MYC2 transcription factor to provide time-of-day regulation of jasmonate signaling in *Arabidopsis*. Plant Cell **24**:2470–2482.

Straus, M.R., Rietz, S., Ver Loren van Themaat, E., Bartsch, M., and Parker, J.E. (2010). Salicylic acid antagonism of EDS1-driven cell death is important for immune and oxidative stress responses in *Arabidopsis*. Plant J. **62**:628–640.

Stuttmann, J., Peine, N., Garcia, A.V., Wagner, C., Choudhury, S.R., Wang, Y., James, G.V., Griebel, T., Alcazar, R., Tsuda, K., et al. (2016). *Arabidopsis thaliana* DM2h (R8) within the Landsberg RPP1-like resistance locus underlies three different cases of EDS1-conditioned autoimmunity. PLoS Genet. **12**:e1005990.

Thines, B., Katsir, L., Melotto, M., Niu, Y., Mandaokar, A., Liu, G., Nomura, K., He, S.Y., Howe, G.A., and Browse, J. (2007). JAZ repressor proteins are targets of the SCF(COI1) complex during jasmonate signalling. Nature **448**:661–665.

Tsuda, K., and Somssich, I.E. (2015). Transcriptional networks in plant immunity. New Phytol. **206**:932–947.

Tsuda, K., Sato, M., Stoddard, T., Glazebrook, J., and Katagiri, F. (2009). Network properties of robust immunity in plants. PLoS Genet. **5**:e1000772.

Van der Does, D., Leon-Reyes, A., Koornneef, A., Van Verk, M.C., Rodenburg, N., Pauwels, L., Goossens, A., Korbes, A.P., Memelink, J., Ritsema, T., et al. (2013). Salicylic acid suppresses jasmonic acid signaling downstream of SCFCOI1-JAZ by targeting GCC promoter motifs via transcription factor ORA59. Plant Cell **25**:744–761.

Wagner, S., Stuttmann, J., Rietz, S., Guerois, R., Brunstein, E., Bautor, J., Niefind, K., and Parker, J.E. (2013). Structural basis for signaling by exclusive EDS1 heteromeric complexes with SAG101 or PAD4 in plant innate immunity. Cell Host Microbe **14**:619–630.

Wiermer, M., Feys, B.J., and Parker, J.E. (2005). Plant immunity: the EDS1 regulatory node. Curr. Opin. Plant Biol. **8**:383–389.

Wildermuth, M.C., Dewdney, J., Wu, G., and Ausubel, F.M. (2001). Isochorismate synthase is required to synthesize salicylic acid for plant defence. Nature **414**:562–565.

Wirthmueller, L., Zhang, Y., Jones, J.D., and Parker, J.E. (2007). Nuclear accumulation of the *Arabidopsis* immune receptor RPS4 is necessary for triggering EDS1-dependent defense. Curr. Biol. **17**:2023–2029.

Yang, D.L., Yao, J., Mei, C.S., Tong, X.H., Zeng, L.J., Li, Q., Xiao, L.T., Sun, T.P., Li, J., Deng, X.W., et al. (2012). Plant hormone jasmonate prioritizes defense over growth by interfering with gibberellin signaling cascade. Proc. Natl. Acad. Sci. USA **109**:E1192–E1200.

Yang, L., Teixeira, P.J., Biswas, S., Finkel, O.M., He, Y., Salas-Gonzalez, I., English, M.E., Epple, P., Mieczkowski, P., and Dangl, J.L. (2017). *Pseudomonas syringae* type III effector HopBB1 promotes host transcriptional repressor degradation to regulate phytohormone responses and virulence. Cell Host Microbe **21**:156–168.

Yoo, S.D., Cho, Y.H., and Sheen, J. (2007). *Arabidopsis* mesophyll protoplasts: a versatile cell system for transient gene expression analysis. Nat. Protoc. **2**:1565–1572.

Zhai, Q., Yan, L., Tan, D., Chen, R., Sun, J., Gao, L., Dong, M.Q., Wang, Y., and Li, C. (2013). Phosphorylation-coupled proteolysis of the transcription factor MYC2 is important for jasmonate-signaled plant immunity. PLoS Genet. **9**:e1003422.

Zhang, L., Yao, J., Withers, J., Xin, X.F., Banerjee, R., Fariduddin, Q., Nakamura, Y., Nomura, K., Howe, G.A., Boland, W., et al. (2015). Host target modification as a strategy to counter pathogen hijacking of the jasmonate hormone receptor. Proc. Natl. Acad. Sci. USA **112**:14354–14359.

Zhang, X., Bernoux, M., Bentham, A.R., Newman, T.E., Ve, T., Casey, L.W., Raaymakers, T.M., Hu, J., Croll, T.I., Schreiber, K.J., et al. (2017). Multiple functional self-association interfaces in plant TIR domains. Proc. Natl. Acad. Sci. USA **114**:E2046–E2052.

Zheng, X.Y., Spivey, N.W., Zeng, W., Liu, P.P., Fu, Z.Q., Klessig, D.F., He, S.Y., and Dong, X. (2012). Coronatine promotes *Pseudomonas syringae* virulence in plants by activating a signaling cascade that inhibits salicylic acid accumulation. Cell Host Microbe **11**:587–596.

Zhu, Z., Xu, F., Zhang, Y., Cheng, Y.T., Wiermer, M., Li, X., and Zhang, Y. (2010). *Arabidopsis* resistance protein SNC1 activates immune responses through association with a transcriptional corepressor. Proc. Natl. Acad. Sci. USA **107**:13960–13965.